Article

Ligand Binding and Functional Selectivity of L-Tryptophan Metabolites at the Mouse Aryl Hydrocarbon Receptor (mAhR)

Roberto Nuti,[‡] Marco Gargaro,[‡] Davide Matino,[‡] Daniela Dolciami,[†] Ursula Grohmann,[‡] Paolo Puccetti,[‡] Francesca Fallarino,[‡] and Antonio Macchiarulo*[,†]

[†]Department of Pharmaceutical Sciences and [‡]Department of Experimental Medicine, Università di Perugia, via del Liceo 1, 06123 Perugia, Italy

S *Supporting Information*

ABSTRACT: The aryl hydrocarbon receptor (AhR) is a nuclear receptor regulating a wide range of biological and toxicological effects. Metabolites of L-tryptophan are able to bind and activate AhR, providing a link between tryptophan catabolism and a novel mechanism of protective tolerance, referred to as "disease tolerance". The notion that pharmacologic modulation of genes associated with endotoxin tolerance would be beneficial in clinical settings dominated by acute hyper-inflammatory responses to infection thrusts AhR into the limelight as an interesting druggable target. Combining homology modeling, docking studies, and molecular dynamic simulations with mutagenesis experiments and gene profiling, in this work we report that 2,3,7,8-tetrachlorodibenzo-*p*-dioxin (TCDD) and two different L-tryptophan metabolites, namely L-Kynurenine and FICZ (6-formylindolo[3,2-*b*]carbazole), are able to bind to mAhR, exploiting different key interactions with distinct set of fingerprint residues. As a result, they stabilize different conformations of mAhR that, in turn, selectively regulate downstream signaling and transcription of specific target genes. Collectively, these results open new avenues for the design and development of selective AhR modulators that, by targeting specific receptor conformations associated with specific AhR functions, may offer novel therapeutic opportunities in infectious diseases and other morbidity that may be associated with the receptor.
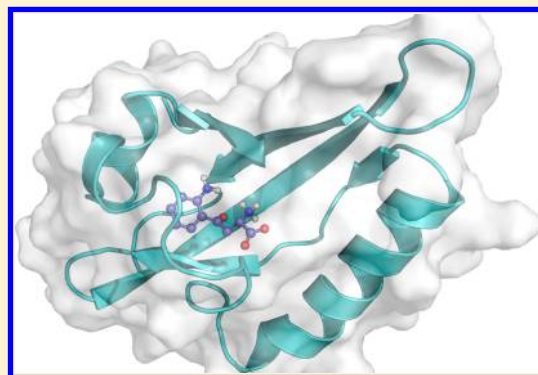
INTRODUCTION

The aryl hydrocarbon receptor (AhR) is a ligand-dependent transcription factor belonging to the basic helix–loop–helix Per-Arnt-Sim (bHLH/PAS) family and regulating a wide range of biological as well as toxicological effects.[1,2] Unlike common nuclear receptors, the functional core of AhR is constituted of two PAS domains, namely PAS-A and PAS-B motifs, and one N-terminal DNA binding bHLH domain.[3] The bHLH domain contains a nuclear localization signature (NLS) that is responsible for the nuclear translocation of AhR. While the PAS-A domain is involved in the formation of the heterodimer with ARNT (AhR nuclear translocator), the PAS-B domain holds one binding cleft for the Heat shock protein 90 (Hsp90) and one ligand binding site with overlapping critical residues.[4]

As far as it concerns the activation of AhR, termed transformation, ligand binding to the PAS-B domain triggers major conformational changes that spread along the entire sequence of the receptor.[5] As a consequence, AhR activates complex and diverse ligand-dependent signaling events through classical and nonclassical mechanisms of action, with differences in sensitivity and response existing among human and animal species.[6,7] Although the molecular basis of AhR transformation is still elusive, some authors have proposed that conformational changes occurring upon ligand binding first allow the protein to expose the NLS to favor nuclear translocation and ARNT

dimerization.[8,9] Others, however, have suggested that ligand binding to the receptor promotes conformational changes which raise the solvent exposure of PAS-A, displacing Hsp90 from PAS-B and ultimately leading to the formation of AhR/ARNT heterodimer and AhR transformation.[4,10]

AhR is a promiscuous receptor, with its activation being regulated by structurally different ligands that include environmental pollutants such as 2,3,7,8-tetrachlorodibenzo-*p*-dioxin (TCDD), related halogenated aromatic hydrocarbons (HAHs) and polycyclic aromatic hydrocarbons (PAHs).[11,12] FICZ (6-formylindolo[3,2-*b*]carbazole), a photoproduct of L-trypto-phan,[13] is another ligand that modulates AhR, showing a higher binding affinity to the receptor than TCDD.[14]

Of note, a comparative study between AhR-mediated activations of TCDD and FICZ in a mouse model of influenza virus infection reported differences in the immunomodulatory actions of the two ligands, with these being ascribed to the duration of AhR activation and cell types in which the receptor activation occurred.[15] More recently, site-directed mutagenesis identified Ile319 as an important binding site residue for the agonistic activity of FICZ in mouse AhR.[16]

L-Kynurenine (L-Kyn) has been reported as an endogenous ligand for AhR, regulating T-cell differentiation, and inducing immunosuppressant effects in cancer cells.[17,18] L-Kyn is a key metabolite of the main route of L-tryptophan catabolism, wherein it is used as substrate for the formation of the neuroprotective Kynurenic acid (KYNA) or the neurotoxic Quinolinic acid (QUINA) along two branches of the Kynurenine pathway.[19,20] Remarkably, L-Kyn has also been shown to act as chemical messenger in disease tolerance pathways, linking tryptophan catabolism to the activation of the AhR signaling cascade.[21]

According to the paradigm that high receptor flexibility is correlated to ligand promiscuity as well as functional selectivity,[22,23] different conformations of AhR PAS-B domain may favor the binding of structurally distinct ligands and/or coregulator proteins. Accordingly, upon interaction with ligands and either cytosolic binding partners (e.g., Hsp90, XAP2, p23) or nuclear binding partners (e.g., ARNT), the conformational energy landscape of the AhR would change by shifting the equilibrium population and favoring the presence of specific conformational states of the receptor that may account for its transformation and the regulation of specific downstream signaling pathways and/or expression of target genes.

While several crystallographic studies and NMR spectroscopy of distant homologous PAS-containing proteins have been instrumental to unveil common folding properties of this structural unit,[24−30] homology models of the PAS-B AhR domain have provided frameworks for its structural and functional characterization.[31−33] Specifically, early models of PAS-B AhR domain were based on the structures of the conserved PAS-B motifs of human hypoxia-inducible factor 2α (HIF-2α)[25] and human ARNT protein.[29] Although these models proved successful to identify residues involved in the binding of TCDD to the receptor as well as functional diversity of mutant AhR,[34,35] they have limitations for molecular docking approaches, being derived from apo template structures.[36] Crystallization studies of the heterodimer complex between PAS-B HIF-2α and PAS-B ARNT in the absence and presence of different small molecules,[28] while providing further insights into the energetic and conformational aspects of ligand binding to the receptor, have allowed the generation of improved homology models of PAS-B AhR for the study of the ligand binding mode.[37,38]

Based on these observations, in the first part of the study we report a computational study aimed at revealing the binding modes of FICZ and L-Kyn to the PAS-B domain of mAhR and comparing them with that of TCDD. In the second part of the work, experimental appraisals are carried out to assess potential links between different ligand-bound conformations of mAhR and specific gene regulations.

■ MATERIALS AND METHODS

Chemicals. L-Kynurenine (L-Kyn) and 2,3,7,8-tetrachlorodibenzo-*p*-dioxin (TCDD) were purchased from Sigma-Aldrich Supelco, and 6-Formylindolo (3,2-b) carbazole (FICZ) was purchased from Biomol (Plymouth Meeting, PA).

Homology Modeling. Homology modeling was applied to build the structure of mouse PAS-B AhR (mAhR residues 278−384). The amino acid sequence of the receptor was obtained from the NCBI database (accession number NP_038492.1). A multiple alignment between the sequences of PAS-B AhR and PAS-B HIF-2α was generated according to the alignment suggested by Pandini and co-workers.[31,34] Using Modeler, three

homology models of PAS-B AhR were thus constructed on the templates of PAS-B HIF-2α, as retrieved from the crystal structures of the receptor in the absence and presence of ligands (pdb codes 3f1p, 3f1o, 3f1n).[39] A fourth model was produced using a multitemplate strategy. As implemented in Modeler, this strategy consists in generating a homology model combining the three template structures according to the sequence alignment between all of the templates and the PAS-B mAhR. For each procedure, 200 structural solutions of the receptor were built and the model with the lowest energy was selected (models a−d). It should be mentioned that we did not used the technique mentioned in ref 37 in which the structures of the ligands are transferred into the homology models during modeling and refinement stages to obtain a binding cavity that takes into account ligand induced-fit effects. This is because the chemical structure of the ligand in 3f1o, namely *N*-[2-nitro-4-(trifluoromethyl)phenyl]morpholin-4-amine (Figure S1, Supporting Information), is different from L-Kyn, TCDD, and FICZ. Accordingly, keeping this compound during modeling and refinement stages of homology models would have introduced a bias in the ligand induced-fit effects toward a specific chemical class of AhR ligands. Models a−d were submitted to the protein preparation refinement protocol as implemented in Maestro v.9.7 (Schrödinger, LLC, New York, NY, 2014), consisting of the optimization of the hydrogen bond network followed by a restrained energy minimization using the OPLS-2005 force field with a maximum allowed root-mean-square deviation (RMSD) of 0.30 Å for $C\alpha$ atoms. The quality of the models was assessed by different statistical methods, including Verify3D, Procheck, and Molprobity.[40−42] SiteMap (Schrödinger, LLC, New York, NY, 2014) was instrumental in defining the binding site and calculating binding site descriptors for each of the four models of PAS-B AhR. Specifically, four binding site descriptors were calculated including and druggability score (D-score), volume (vol), hydrophobic character (phobic), and hydrophilic character (philic).[43]

Docking Studies and Molecular Dynamics (MD). The chemical structures of TCDD, L-Kyn, and FICZ were generated using LigPrep v.2.9 (Schrödinger, LLC, New York, NY, 2014). For each ligand, we considered different tautomeric and ionization states at the physiological pH of 7.0. The geometry of the compounds was refined using DFT/6-31G** calculations with Jaguar v.8.3 (Schrödinger, LLC, New York, NY, 2014).[44]

Docking studies into the four models of PAS-B AhR were performed employing the quantum mechanics-polarized ligand docking (QPLD) workflow and Glide v.6.2 (Schrödinger, LLC, New York, NY, 2014).[45] According to this workflow, ligand atomic partial charges are calculated using a QM/MM approach, with the B3LYP method and the 6-31G* basis set, and fitting the electrostatic potential (ESP). Docking poses were obtained employing Glide extra precision mode (XP). For each ligand, the best scored pose obtained by comparing docking solutions among the four models was selected for molecular dynamics (MD). MD simulations allow taking into account ligand induced-fit effects, providing a thorough analysis of conformational changes induced by L-Kyn, TCDD, and FICZ binding to PAS-B AhR. The three selected PAS-B AhR ligand bound complexes from QPLD docking studies were then solvated in an orthorhombic box using TIP3P water molecules, extended 10 Å away from any protein atom. Each of the resulting three systems was neutralized by adding sodium and

chlorine ions at a concentration of 0.15 M. Periodic boundary conditions were applied to avoid finite-size effects. Atomic partial charges of ligands were maintained as obtained from QPLD calculation. MD simulations were performed using Desmond v.2.4 and the OPLS-2005 force field. The simulation protocol included starting relaxation steps and a final production phase of 50 ns. In particular, relaxation steps comprised an initial energy minimization of the system over a maximum 2000 steps, with a convergence criterion of 50 kcal/mol Å, and the presence of harmonic restraints on the solute atoms (force constant = 50.0 kcal/mol Å^2); a second energy minimization without restraints; a third stage of 12 ps at 10 K with harmonic restraints on the solute heavy atoms (force constant = 50.0 kcal/mol Å^2), using the *NVT* ensemble and Berendsen thermostat; a fourth 12 ps at 10 K, retaining the harmonic restraints, and using the *NPT* ensemble and Berendsen thermostat and barostat; a fifth heating phase of 24 ps at 300 K, retaining the harmonic restraints, and using the *NPT* ensemble and Berendsen thermostat and barostat; a final 24 ps at 300 K without harmonic restraints, using the *NPT* Berendsen thermostat and barostat. The final production phase of MD was run using a canonical the NPT Berendsen ensemble at temperature 300 K. During MD simulations, we used a time step of 2 fs while constraining the bond lengths of hydrogen atoms with the M-SHAKE algorithm.[46] The atomic coordinates were saved every 4.8 ps. The occupancy of intermolecular hydrogen bonds, aromatic interactions, and hydrophobic contacts were calculated along the last 48 ns of the production phase of each MD simulation, using a cutoff value of 30% and the Simulation Interaction Diagram Tools implemented in Maestro v.9.7.

Luciferase Reporter Assay. AhR-deficient cDCs (10 × 106), reconstituted either with WT or Gln377Ala AhR, were electroporated (230 V, 75 Ohm, and 1500 microfarads) in Optimem/Glutamax (Invitrogen) with 30 μg of the firefly luciferase reporter pGudLuc1.1 plasmid, which contains a 480 bp fragment of the upstream enhancer region of the mouse Cyp1a1 gene—including four xenobiotic response elements—upstream of the firefly luciferase coding sequence. Another reporter plasmid, pRL-TK (1 μg; Promega) encoding Renilla luciferase, was electroporated as an internal control of the transfection process. Cells were seeded in 24-well plates at a density of 1.2 × 10^6 cells/mL. After 2 h at 37 °C, cells were stimulated for 8−10 h with increasing concentrations of TCDD or FICZ, as the reference AhR ligands, or L-Kyn before lysis. Luciferase assays were performed using the dual luciferase reporter assay kit (Promega).

Isolation Dendritic Cells and Treatments. Splenic DCs were purified using CD11c MicroBeads (Miltenyi Biotec) in the presence of EDTA to disrupt DC-T cell complexes. Cells were >99% CD11c+, >99% MHC I-A+, >98% B7-2+, <0.1% CD3+, and appeared to consist of 90−95% CD8−, 5−10% CD8+, and 1−5% B220+ cells. For in vitro studies, DCs (1 × 10^6 cells per well in 24-well plates) were cultured for 24 h with medium or with AhR ligands at specific doses for 24 h and assessed for gene expression by Real-Time RT-PCR.

Real-Time RT-PCR. Real-Time RT-PCR (for mouse *Cyp1a1*, *Cyp1b1*, *Il10*, *Tgfb1*, and *Gapdh*) analyses were carried out as described in ref 21, using the specific primers listed: *Gapdh* 5′-GCC TTC CGT GTT CCT ACC C-3′, 5′-CAG TGG GCC CTC AGA TGC-3; *Cyp1a1* 5′-GAC ACA GTG ATT GGC AGA G-3′, 5′-GAA GGT CTC CAG AAT GAA GG-3; *Cyp1b1* 5′-CTG CCA CTA TTA CGG ACA T-3, 5′-

GGG TAT CTG GTA AAG AGG ATG-3; *Tgfb1* 5′-CAC AGA GAA GAA CTG CTG TG-3′, 5′-AGG AGC GCA CAA TCA TGT TG-3′; *Il10* 5′-ACC AGC TGG ACA ACA TAC TG-3′; 5′-CGC ATC CTG AGG GTC TTC AG-3′. In all figures depicting RT-PCR data, bars represent the ratio of gene to Gapdh expression, as determined by the relative quantification method ($\Delta\Delta$CT; means ± s.d. of triplicate determination). In FACS analyses, cells were treated with rat anti-CD16/32 (2.4G2) for 30 min at 4 °C for blocking of Fc receptors before assaying on a LSRFortessa (BD BioSciences) flow cytometer for AhR expression and analyzed by flowJo data analysis software.

Statistical Analysis. All in vitro determinations are means ± s.d. from three independent experiments and were evaluated by the Shapiro test and Student's *t* test, as appropriate. All *n* values were computed by power analysis to yield a power of at least 80% with an α-level of 0.05. GraphPad Prism version 6.0 (San Diego, CA) was used for all analyses.

■ RESULTS

Homology Modeling of PAS-B AhR. Four homology models of PAS-B AhR (models a−c, Table 1) were generated

Table 1. Homology Models of PAS-B AhR and Statistical Values

model	template (PDB code)	resolution (Å)	residues in favored Ramachandran regions (%)	verify 3D max−min values
a	3F1P	1.17	85.7%	0.53−0.22
b	3F1O	1.48	91.4%	0.54−0.15
c	3F1N	1.60	88.6%	0.51−0.16
d	3F1N 3F1O 3F1P		90.5%	0.55−0.12

using the crystal structures of HIF2α and following the computational procedure reported in the Materials and Methods section. Aligning the structures of the four homology models on their Cα atoms, they do not show any apparent difference between their backbone conformations, with the exception of the loop connecting β-sheets H and I (residues 366−370, Figure 1). Conversely, different properties of the ligand binding cleft are observed in each model, suggesting the presence of diverse side chain conformational rearrangements of binding site residues (Table 2).

In particular, the ligand binding cavities of model **a** and **c** show a smaller size with largely hydrophobic properties, whereas those of models **b** and **d** feature a larger size with more hydrophilic properties. Each of the four models of PAS-B AhR thus represents a specific conformation of the ligand binding cavity, suitable to accommodate the ligands with different physicochemical properties.

Binding Modes of TCDD, FICZ, and L-Kyn to PAS-B AhR. Docking studies and MD simulations were performed to study the binding modes of tryptophan metabolites to PAS-B AhR compared to that of TCDD. As a result of docking studies, TCDD, FICZ, and L-Kyn show the binding pose with the best energy score when docked into model **c**, **a**, and **d**, respectively (Table 3). Hence, ligands with different properties fit diverse models of the binding cleft of PAS-B AhR.

In order to optimize the binding energies of these ligand/receptor complexes, taking into account possible ligand-
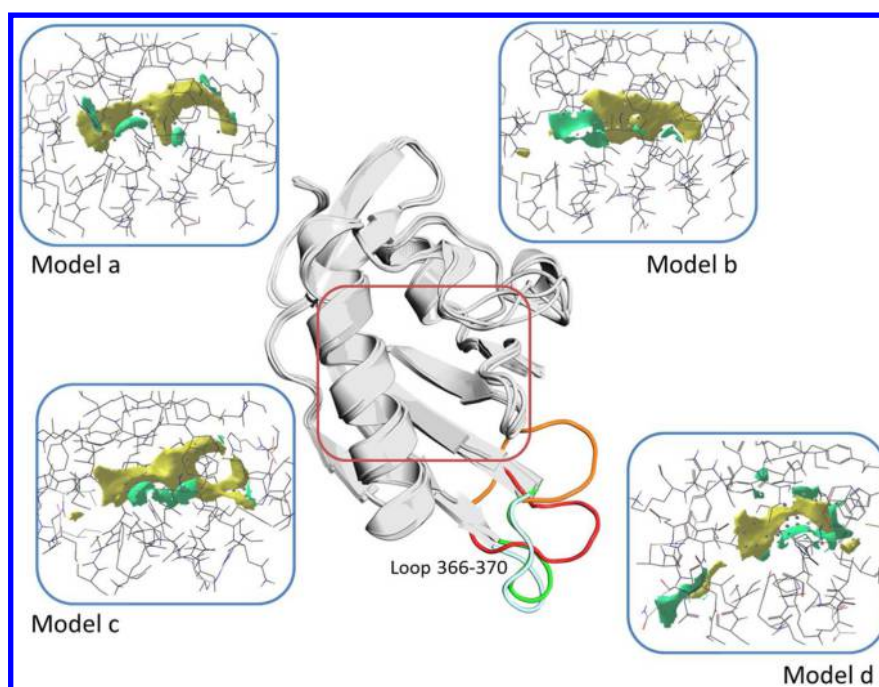
Figure 1. Structural alignment of the four homology models (a–d) of PAS-B AhR on the Cα atoms. Conformations of the loop connecting β-sheets H and I are color coded in cyan (model a), red (model b), orange (model c), and green (model d). In the boxes, hydrophilic (green contour surface) and hydrophobic (yellow contour surface) properties of binding site are shown for each of the four models.
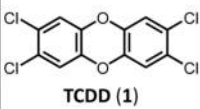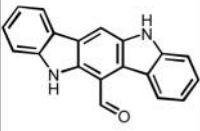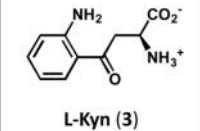
Table 2. Properties of the Binding Site of PAS-B AhR Models

model	D-score	vol (Å³)	phobic	philic
a	1.34	142	4.23	0.51
b	1.15	195	2.61	0.89
c	1.29	170	3.72	0.67
d	1.15	177	2.15	1.12

induced fit effects, MD simulations of 50 ns were carried out on ligand bound PAS-B AhR complexes in a full water solvated box. The inspection of RMSD values of backbone atoms of the receptor along the MD trajectories of the complexes shows that the each system reaches a plateau of stabilization after the initial 15 ns of the simulations (Figure 2a).

The analysis of RMSD values of TCDD (RMSD = 3.52 ± 0.90 Å), FICZ (RMSD = 1.79 ± 0.70 Å), and L-Kyn (RMSD =

Table 3. Properties (SASA; Calculated Octanol/Water Partition Coefficient, cLogP) and Top Docking Scores of TCDD, FICZ, and L-Kyn into Models of PAS-B AhR

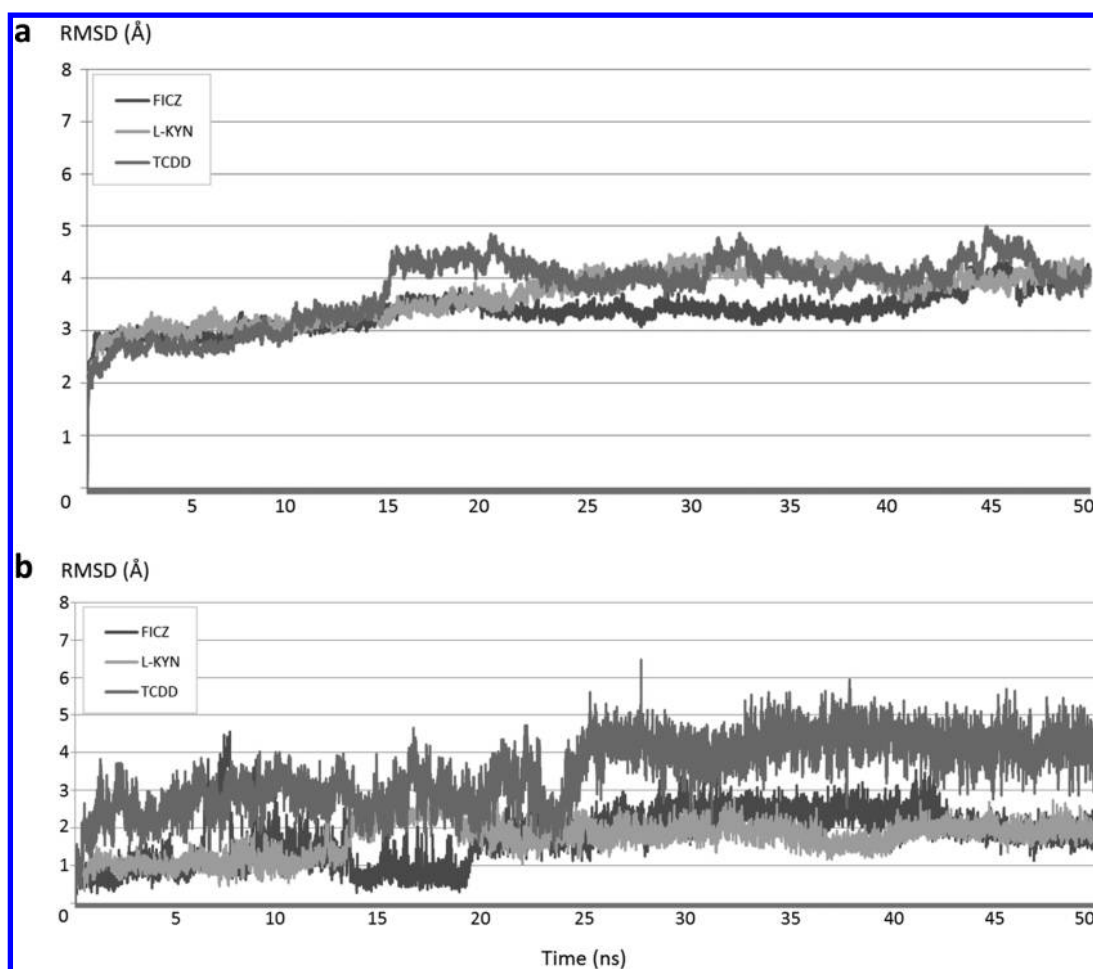| Ligand	cLogP	SASA[a] (Å²)	Model a XP Score (kcal/mol)	Model b XP Score (kcal/mol)	Model c XP Score (kcal/mol)	Model d XP Score (kcal/mol)
TCDD (1)	6.4	474	-7.80	-4.58	-8.81	-6.44
FICZ (2)	4.1	521	-8.72	-6.06	-7.56	-6.45
L-Kyn (3)	-0.5	387	-5.13	-4.93	-3.76	-6.72

[a]SASA, solvent accessible surface area.

Figure 2. (a) Plot of the RMSD of backbone atoms of PAS-B AhR along the MD trajectory (50 ns) for FICZ bound AhR complex (black line), L-Kyn bound AhR complex (light gray line), and TCDD bound AhR complex (gray line). (b) Plot of the RMSD of heavy atoms of ligand along the MD trajectory (50 ns) for FICZ (black line), L-Kyn (light gray line), and TCDD (gray line).

1.71 ± 0.47 Å) shows that TCDD undergoes to a major drift after the first 25 ns of the simulation (Figure 2b). Then, it remains stably bound to the receptor until the end of 50 ns. Conversely, FICZ and L-Kyn undergoes minor fluctuations for the entire simulation, with the former ligand showing some unstable drifts in a window between the 5 and 9 ns. Each compound features specific interactions with binding site residues. Specifically, TCDD engages aromatic and hydrophobic residues (His285, Phe289, Phe345, Met342) with stable π-stacking interactions and favorable van der Waals contacts (occupancy >30%), respectively. Analyzing the course of these interactions along the trajectory (Figure 3a), TCDD forms one hydrogen bond between one of its oxygen atom and the side chain of Gln377 during the first part of the simulation (from time 0 to ~25 ns, occupancy 33%). Thereafter, this polar interaction breaks due to a conformational rearrangement of binding site residues, resulting in the formation of a more stable hydrophobic packing with Met342 and Phe345 (Figure 3b and c). The binding of FICZ to PAS-B AhR is stabilized through π-stacking interactions (His285), a number of hydrophobic contacts (Phe289, Tyr316, Ile319, Phe345, Leu347), and hydrogen bonds (Gly315, Ser359, Gln377) (Figure 4a). Concerning polar interactions, while the aldehyde moiety of FICZ makes two hydrogen bonds with the side chains of Ser359 (occupancy 62%) and Gln377 (occupancy 93%), the indolic nitrogen atoms engage Gly315 (occupancy 78%) and

Gln377 (occupancy 30%) with two additional hydrogen bonds (Figure 4b and c). L-Kyn is the smallest ligand among the above studied compounds and the most hydrophilic, bearing an amino acidic zwitterionic moiety. It shows a different pattern of binding interactions compared to TCDD and FICZ, mostly characterized by a large number of polar interactions over hydrophobic and π-stacking contacts (Figure 5a). Specifically, the carboxylic group of L-Kyn forms two hydrogen bonds with the backbone of Tyr316 (occupancy 77%) and Phe318 (occupancy 62%). The α-amino moiety interacts through a π-cation stacking with Phe289 and one hydrogen bond with His285 (occupancy 85%). Additional stable hydrogen bonds are observed between the carbonyl and aniline groups of L-Kyn and the side chains of Gln377 (occupancy 79%) and Thr283 (occupancy 73%) (Figure 5b and c). Only a few stable hydrophobic contacts (occupancy >30%) are observed during the MD trajectory of L-Kyn bound to PAS-B AhR, with these contacts involving the benzene ring of L-Kyn and the side chains of Pro291 and Leu302. An overlap of the binding modes of the three ligands to PAS-B mAhR as resulting from MD simulations is provided in Figure S2 of the Supporting Information.

Mutagenesis Experiments and Gene Expression Profiling. On the basis of the results from docking and MD simulations, a mutant AhR receptor was engineered carrying a Gln377Ala mutation (Q377A), and AhR-deficient DCs were
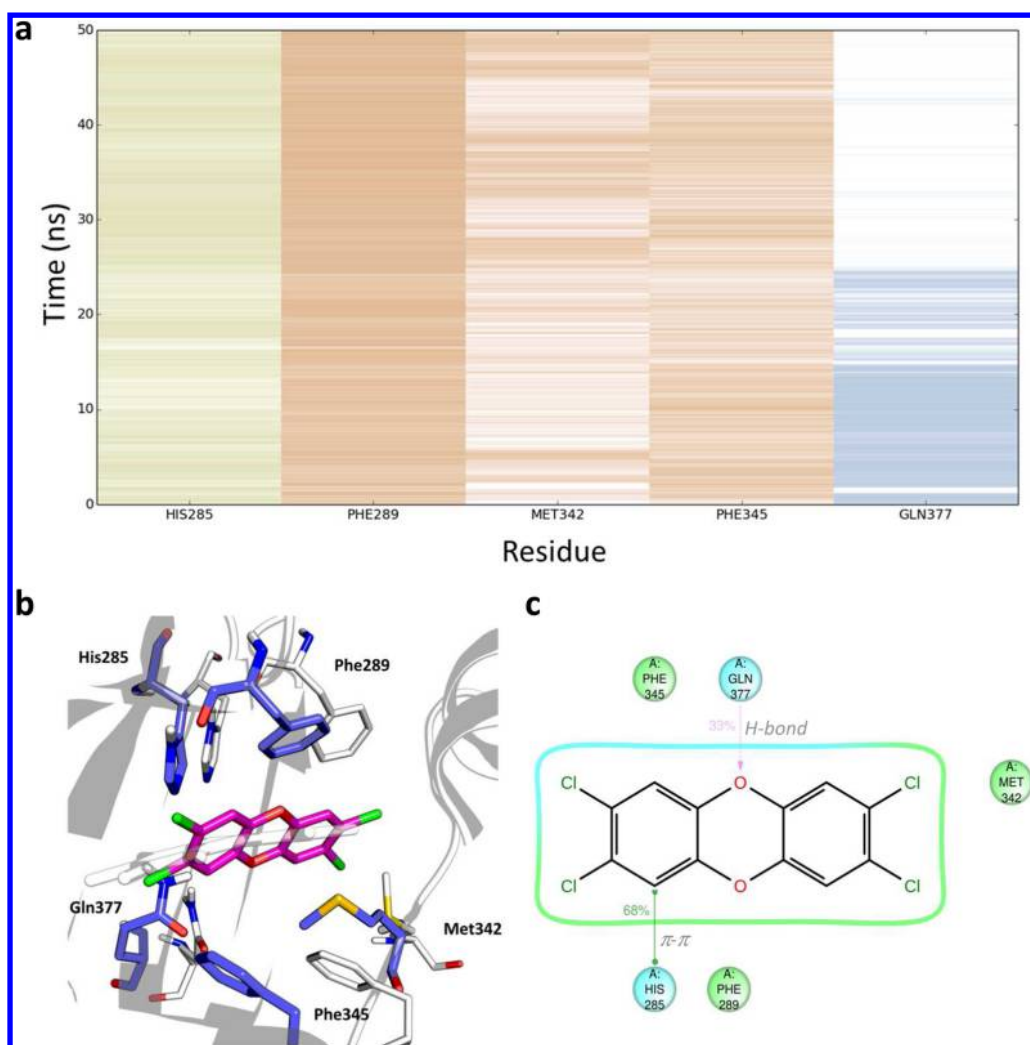
Figure 3. (a) Heat map of polar (blue lines), hydrophobic (brown lines), and aromatic (green line) contact interactions of binding site residues with TCDD along the MD trajectory (50 ns). (b) Binding mode of TCDD to PAS-B AhR at the end of MD simulation (purple and blue carbon sticks) superimposed on the one resulting from the docking study (white carbon sticks). (c) Cartoon graph showing the interactions of TCDD with binding site residues along with relative occupancies.

reconstituted with AhR[WT] or AhR[Gln377Ala]. Transfection efficiency was similar for the two constructs, as revealed by staining with antibody recognizing both AhR[WT] and mutant AhR[Gln377Ala] on FACS analysis (data not shown). When assayed in a luciferase reporter assay using mouse dendritic cells (DCs) reconstituted with mutated AhR[Gln377Ala], L-Kyn exhibits a complete loss of biologic activity, in terms of potency and likely affinity, compared to AhR[WT] transfected counterparts (Figure 6a). In contrast, while no difference could be detected for FICZ (Figure 6b), on stimulation with TCDD, the 50% maximal effective concentration (EC_{50}) value of TCDD is approximately 20-fold lower when cells were reconstituted with the mutant receptor (Figure 6c), pointing to greater potency and affinity of the ligand for AhR[Gln377Ala].

In order to evaluate the impact of AhR activation by the three different ligands (TCDD, FICZ, or L-Kyn) on transcriptional gene expression in DCs, AhR-deficient mouse splenic DCs were reconstituted with AhR[WT] or AhR[Gln377Ala] and assessed for *Cyp1a1* (Figure 7a), *Cyp1b1* (Figure 7b), transforming growth factor-β (*Tgfb1*, Figure 6c) and indoleamine 2,3-dioxygenase 1 (*Ido1*, Figure 7d) quantitative expression, as prototype genes for drug-metabolizing enzymes

(*Cyp1a1*, *Cyp1b1*) or immunoregulatory factors (*Tgfb1* and *Ido1*). Interestingly, in a dose-dependent manner, L-Kyn mostly promotes expression of the anti-inflammatory genes *Tgfb1* and *Ido1*, while the other two ligands TCDD or FICZ are mostly effective in inducing the drug-metabolizing enzymes *Cyp1a1* or *Cyp1b1*. Moreover, while L-Kyn-mediated AhR transcriptional activity is reduced in cells expressing the mutant AhR[Gln377Ala], such mutation does not impair TCDD or FICZ induced transcriptional activation of AhR.

■ DISCUSSION

AhR is a ligand-dependent transcription factor regulating diverse signaling pathways through classical and nonclassical mechanisms of action. Recently, we have shown that L-tryptophan metabolites are able to bind and activate AhR, providing a link between tryptophan catabolism, disease tolerance pathways and endotoxin tolerance.[21] As a continuation of our study, in this work we have investigated in depth the binding modes of two different L-tryptophan metabolites, namely FICZ and L-Kyn, to the PAS-B domain of mAhR, all also with respect to TCDD, a well characterized ligand of the receptor. Collectively, these molecules are endowed with
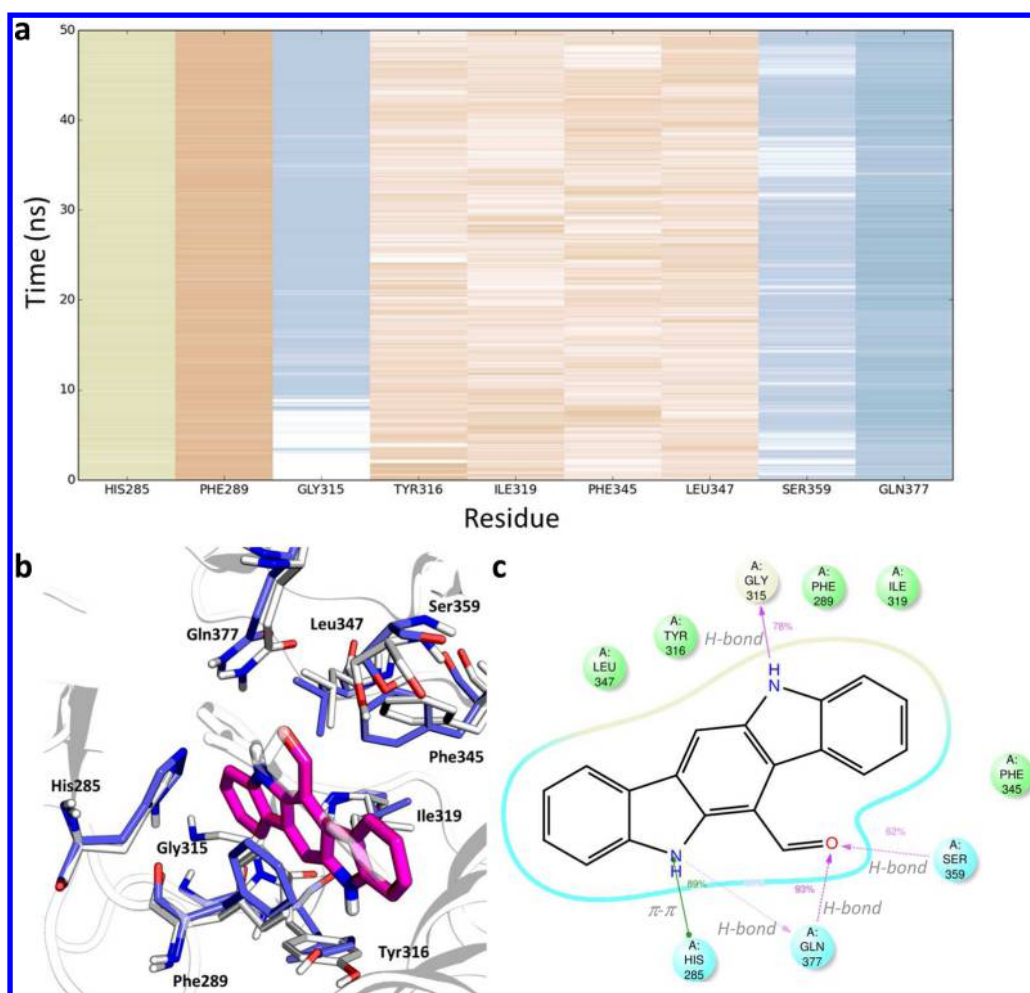
Figure 4. (a) Heat map of polar (blue lines), hydrophobic (brown lines), and aromatic (green line) contact interactions of binding site residues with FICZ along the MD trajectory (50 ns). (b) Binding mode of FICZ to PAS-B AhR at the end of MD simulation (purple and blue carbon sticks) superimposed on the one resulting from the docking study (white carbon sticks). (c) Cartoon graph showing the interactions of FICZ with binding site residues along with relative occupancies.

different physicochemical properties, including size and hydrophobicity (Table 3). L-Kyn is a small and hydrophilic compound; FICZ is a large and quite hydrophilic ligand; TCDD is a large and hydrophobic compound.

Docking studies followed by 50 ns MD simulations show that these molecules fit three different conformations of the AhR binding site, as generated by a multitemplate homology modeling approach. In the resulting complexes, the physicochemical properties of L-Kyn, FICZ, and TCDD match complementary hydrophilic and hydrophobic characters of binding cleft conformations. Of note, different stabilizations of the interaction patterns are observed between each ligand and binding site residues (Figures 3−5). In agreement with the previously reported fingerprint of interacting residues,[34] TCDD is packed with aromatic and hydrophobic residues that include stable contacts (occupancy >30%) with His285, Phe289, Phe345, and Met342. During the second half of the simulation, the conformational rearrangement of some of these residues weakens the hydrogen bond interaction observed between TCDD and Gln377 (Figure 3).

Similarly to TCDD, the binding mode of FICZ to PAS-B AhR involves interactions with aromatic and hydrophobic residues (Figure 4). However, specific hydrogen bond acceptor interactions are also observed between the aldehyde moiety and

the side chains of Ser359 and Gln377, as well as hydrogen bond donor interactions between the indolic nitrogen atoms and the carbonyl groups of Gly315 and Gln377. The binding mode of L-Kyn to AhR is endowed with a different pattern of interactions than TCDD and FICZ, featuring a large number of hydrogen bond interactions that engage Thr283, His285, Tyr316, Phe318, and Gln377 (Figure 5).

Docking studies and MD simulations thus support the ability of TCDD, FICZ, and L-Kyn to interact with diverse PAS-B conformations of AhR, identifying the hydrogen bond with Gln377 as the only conserved polar interaction shared by the three ligands, albeit with different extents of stabilization. To substantiate this in silico observation and investigate further the role of Gln377 in the AhR-mediated transcriptional activity of tryptophan metabolites and TCDD, we engineered the mutant AhR[Gln377Ala] and assessed the levels of luciferase activity in mouse DCs (Figure 6). Three distinct functional behaviors were found: TCDD increases its activity to the mutated receptor of 1 order of magnitude; FICZ keeps potency against AhR[Gln377Ala] similar to the wild type; L-Kyn abolishes its receptor-mediated transcriptional activity. Hence, the hydrogen bond with Gln377 is critical for L-Kyn activity, whereas FICZ and TCDD can compensate for the lack of such interaction with the presence of larger hydrophobic and aromatic contacts
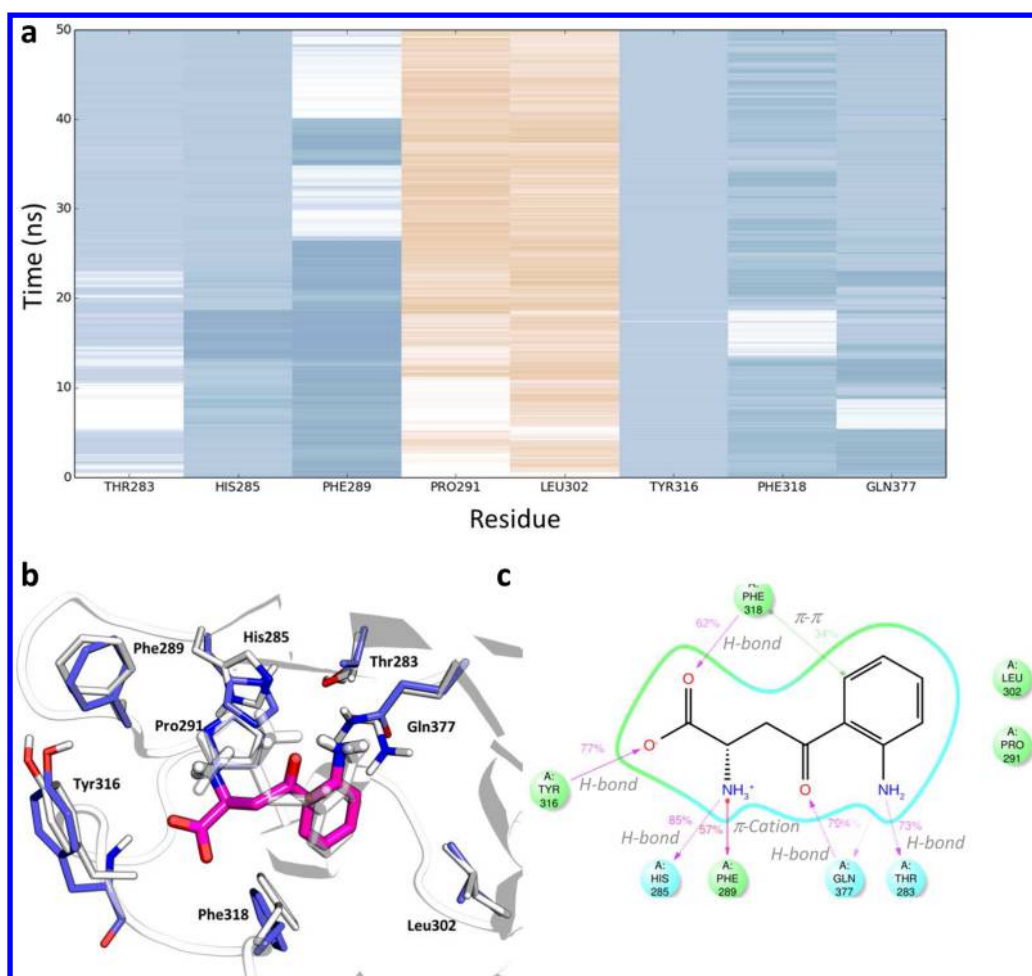
Figure 5. (a) Heat map of polar (blue lines), hydrophobic (brown lines), and aromatic (green line) contact interactions of binding site residues with L-Kyn along the MD trajectory (50 ns). (b) Binding mode of L-Kyn to PAS-B AhR at the end of MD simulation (purple and blue carbon sticks) superimposed on the one resulting from the docking study (white carbon sticks). (c) Cartoon graph showing the interactions of L-Kyn with binding site residues along with relative occupancies.
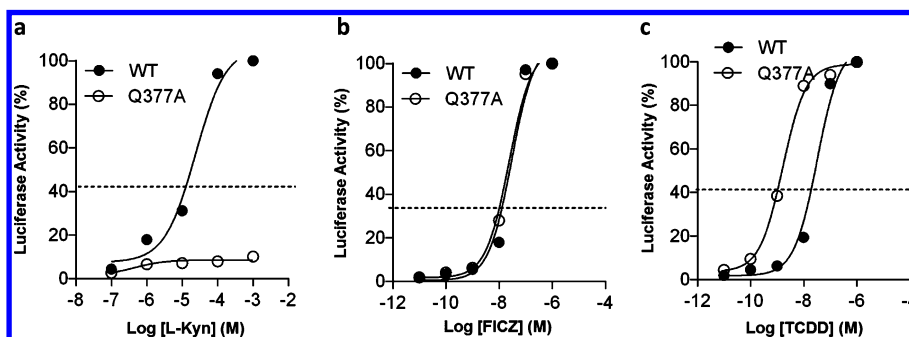

Figure 6. (a) Activity of L-Kyn at wild type (WT) and mutated receptor (Q377A) in the luciferase reporter assay. (b) Activity of FICZ at wild type (WT) and mutated receptor (Q377A) in the luciferase reporter assay. (c) Activity of TCDD at wild type (WT) and mutated receptor (Q377A) in the luciferase reporter assay.

to the receptor. Interestingly, the replacement of a polar residue with a small and hydrophobic one in the AhR[Gln377Ala] favors TCDD activity, likely by enlarging and bestowing more hydrophobic properties to the binding site of the receptor.

It should be mentioned that these data are at odds with the results of binding experiments of TCDD to AhR[Gln377Ala] reported in literature, wherein a 31% of binding to the mutant receptor was observed compared to the wild type mAhR.[31] Nevertheless, such a comparison may suffer from the cellular

assays used in this study and the biochemical assays used in that study, with the formers taking into account also the ability of the mutant receptor to recruit coregulators and to bind to target genes and the latter being based on the binding competition of TCDD to mAhR.

Next, we wondered whether the three different conformations of AhR binding site, as stabilized by TCDD, FICZ, and L-Kyn, could be associated with the selective regulation of downstream signaling by promoting the expression of specific
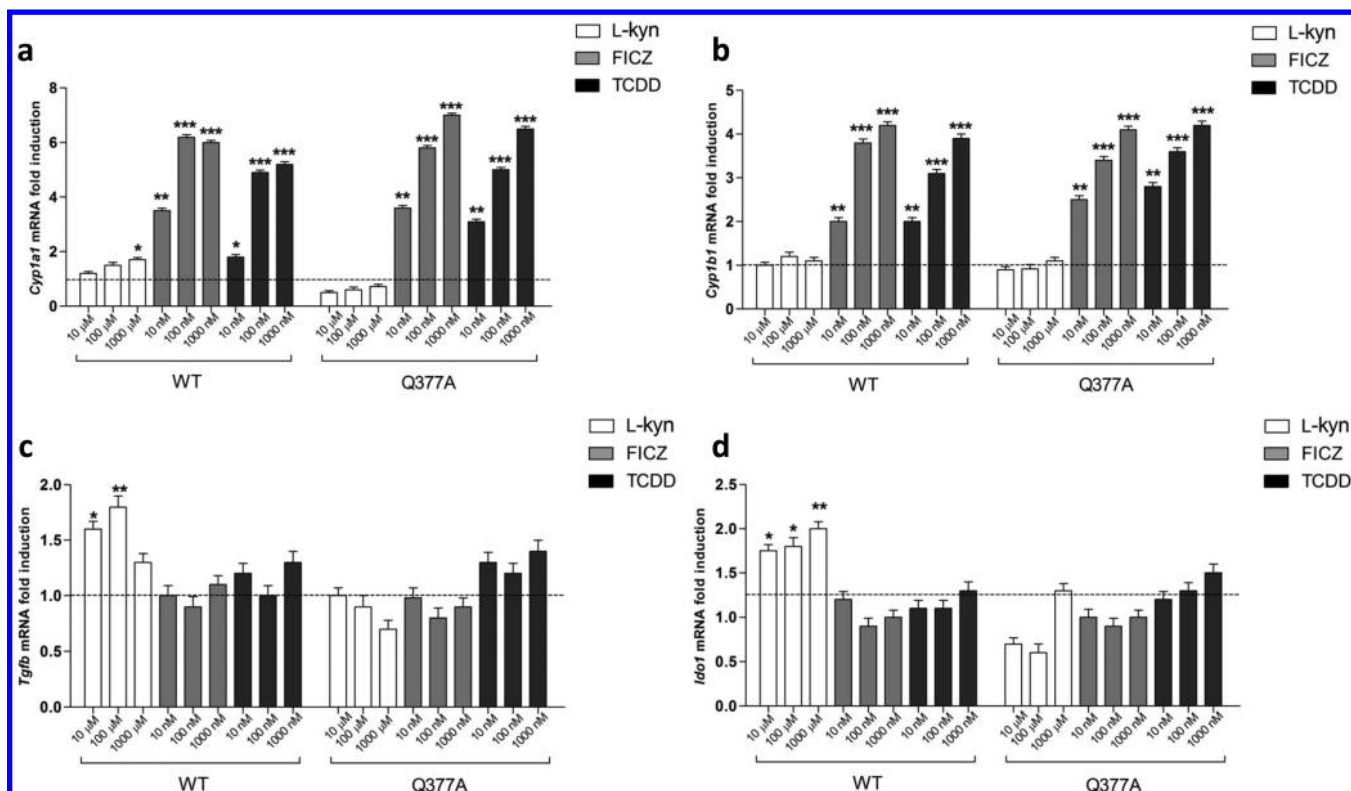
3380

dx.doi.org/10.1021/ci5005459 | J. Chem. Inf. Model. 2014, 54, 3373–3383

Figure 7. AhR mediated transcriptional activity of TCDD, FICZ, and L-Kyn on the regulation of the expression of metabolic target genes [*Cyp1a1* (a) and *Cyp1b1* (b)] and anti-inflammatory genes target [*Tgfb1* (c) and *Ido1* (d)] in DCs expressing AhR^{WT} or AhR^{Gln377Ala}. Means ± s.d. of three experiments. ** $P < 0.05$; *** $P < 0.001$ (Shapiro test).

target genes. The concept of functional selectivity or biased agonism by which ligand-induced receptor conformations can result in differential activation of signal transduction pathways has been observed and discussed mostly for GPCRs and classical nuclear receptors.[23,47−51] In the case of AhR, the concept of selective receptor modulators (SAhRMs) was early introduced by Safe and McDougal[52] and then used to explain alternative AhR transcriptional responses specifically mediated by some other ligands but not TCDD.[53−55]

Accordingly, we compared the AhR mediated transcriptional activity of TCDD, FICZ, and L-Kyn to regulate the expression of canonical target genes such as *Cyp1a1* and *Cyp1b1*, and alternative target genes including *Tgfb1* and *Ido1* in DCs expressing AhR^{WT} or AhR^{Gln377Ala} (Figure 7). As a result, we found that L-Kyn specifically promotes expression of the anti-inflammatory genes *Tgfb1* and *Ido1*, while the other two ligands are mostly effective in inducing the drug-metabolizing enzymes *Cyp1a1* and *Cyp1b1*. Conversely to TCDD and FICZ, the transcriptional activity of L-Kyn on the anti-inflammatory genes was abolished in cells expressing the mutant AhR^{Gln377Ala}. Overall, these results may suggest a mechanistic link between the binding mode of L-Kyn, FICZ, and TCDD to PAS-B AhR, the ensuing specific ligand-induced conformations of the receptor, and eventually the recognition of specific target gene responsive elements. Further work is however needed to prove such hypothesis.

CONCLUSIONS

AhR constitutes the hub of a complex network of regulatory signals that includes the control of drug metabolism and inflammation pathways. Our study shows that TCDD and two L-tryptophan metabolites, namely FICZ and L-Kyn, bind to

different conformations of PAS-B AhR as generated from multitemplate homology modeling. They adopt different binding modes, engaging specific fingerprint residues during MD simulations. Eventually, this results in the stabilization of unique ligand-induced conformations. While in the case of the endogenous metabolite L-Kyn the ligand bound receptor conformation triggers the transactivation of the anti-inflammatory genes *Tgfb1* and *Ido1*, in the case of FICZ and TCDD ligand bound receptor complexes promote the expression of drug-metabolizing enzymes *Cyp1a1* and *Cyp1b1*. Although our results support the notion of selective aryl hydrocarbon receptor modulators (SAhRMs),[52] with diverse ligands and binding modes that differentially activate only a subset of functions of AhR, additional studies are needed to investigate such mechanistic hypothesis. If corroborated, this paves the way to the development of AhR ligands with optimized pharmacological activities for novel therapeutic opportunities in different areas, including infectious and cancer diseases.

ASSOCIATED CONTENT

Ⓢ Supporting Information

Figure S1: the chemical structure of *N*-[2-nitro-4-(trifluoromethyl)phenyl]morpholin-4-amine. Figure S2: overlap of the binding modes of L-Kyn, TCDD, and FICZ to PAS-B mAhR, as resulting from MD simulations. This material is available free of charge via the Internet at http://pubs.acs.org.

AUTHOR INFORMATION

Corresponding Author

*Tel.: +39 075 585 5160. Fax +39 075 585 5114. E-mail: antonio@chimfarm.unipg.it.

3381

dx.doi.org/10.1021/ci5005459 | *J. Chem. Inf. Model.* 2014, 54, 3373−3383

REFERENCES

(1) Schmidt, J. V.; Bradfield, C. A. Ah receptor signaling pathways. *Annu. Rev. Cell Dev. Biol.* **1996**, *12*, 55–89.

(2) Kewley, R. J.; Whitelaw, M. L.; Chapman-Smith, A. The mammalian basic helix-loop-helix/PAS family of transcriptional regulators. *Int. J. Biochem. Cell Biol.* **2004**, *36*, 189–204.

(3) Abel, J.; Haarmann-Stemmann, T. An introduction to the molecular basics of aryl hydrocarbon receptor biology. *Biol. Chem.* **2010**, *391*, 1235–1248.

(4) Soshilov, A.; Denison, M. S. Ligand displaces heat shock protein 90 from overlapping binding sites within the aryl hydrocarbon receptor ligand-binding domain. *J. Biol. Chem.* **2011**, *286*, 35275–35282.

(5) Henry, E. C.; Gasiewicz, T. A. Agonist but not antagonist ligands induce conformational change in the mouse aryl hydrocarbon receptor as detected by partial proteolysis. *Mol. Pharmacol.* **2003**, *63*, 392–400.

(6) Denison, M. S.; Soshilov, A. A.; He, G.; DeGroot, D. E.; Zhao, B. Exactly the same but different: promiscuity and diversity in the molecular mechanisms of action of the aryl hydrocarbon (dioxin) receptor. *Toxicol. Sci.* **2011**, *124*, 1–22.

(7) Guyot, E.; Chevallier, A.; Barouki, R.; Coumoul, X. The AhR twist: ligand-dependent AhR signaling and pharmaco-toxicological implications. *Drug Discovery Today* **2013**, *18*, 479–486.

(8) Ikuta, T.; Eguchi, H.; Tachibana, T.; Yoneda, Y.; Kawajiri, K. Nuclear localization and export signals of the human aryl hydrocarbon receptor. *J. Biol. Chem.* **1998**, *273*, 2895–904.

(9) Lees, M. J.; Whitelaw, M. L. Multiple roles of ligand in transforming the dioxin receptor to an active basic helix-loop-helix/PAS transcription factor complex with the nuclear protein Arnt. *Mol. Cell. Biol.* **1999**, *19*, 5811–5822.

(10) Soshilov, A.; Denison, M. S. Role of the Per/Arnt/Sim domains in ligand-dependent transformation of the aryl hydrocarbon receptor. *J. Biol. Chem.* **2008**, *283*, 32995–3005.

(11) Denison, M. S.; Pandini, A.; Nagy, S. R.; Baldwin, E. P.; Bonati, L. Ligand binding and activation of the Ah receptor. *Chem. Biol. Interact.* **2002**, *141*, 3–24.

(12) Stejskalova, L.; Dvorak, Z.; Pavek, P. Endogenous and exogenous ligands of aryl hydrocarbon receptor: current state of art. *Curr. Drug Metab.* **2011**, *12*, 198–212.

(13) Rannug, U.; Rannug, A.; Sjoberg, U.; Li, H.; Westerholm, R.; Bergman, J. Structure elucidation of two tryptophan-derived, high affinity Ah receptor ligands. *Chem. Biol.* **1995**, *2*, 841–845.

(14) Rannug, A.; Rannug, U.; Rosenkranz, H. S.; Winqvist, L.; Westerholm, R.; Agurell, E.; Grafstrom, A. K. Certain photooxidized derivatives of tryptophan bind with very high affinity to the Ah receptor and are likely to be endogenous signal substances. *J. Biol. Chem.* **1987**, *262*, 15422–7.

(15) Wheeler, J. L.; Martin, K. C.; Resseguie, E.; Lawrence, B. P. Differential consequences of two distinct AhR ligands on innate and adaptive immune responses to influenza A virus. *Toxicol. Sci.* **2014**, *137*, 324–334.

(16) Soshilov, A. A.; Denison, M. S. Ligand promiscuity of aryl hydrocarbon receptor agonists and antagonists revealed by site-directed mutagenesis. *Mol. Cell. Biol.* **2014**, *34*, 1707–19.

(17) Mezrich, J. D.; Fechner, J. H.; Zhang, X.; Johnson, B. P.; Burlingham, W. J.; Bradfield, C. A. An interaction between kynurenine and the aryl hydrocarbon receptor can generate regulatory T cells. *J. Immunol.* **2010**, *185*, 3190–3198.

(18) Opitz, C. A.; Litzenburger, U. M.; Sahm, F.; Ott, M.; Tritschler, I.; Trump, S.; Schumacher, T.; Jestaedt, L.; Schrenk, D.; Weller, M.; Jugold, M.; Guillemin, G. J.; Miller, C. L.; Lutz, C.; Radlwimmer, B.; Lehmann, I.; von Deimling, A.; Wick, W.; Platten, M. An endogenous tumour-promoting ligand of the human aryl hydrocarbon receptor. *Nature* **2011**, *478*, 197–203.

(19) Stone, T. W.; Darlington, L. G. Endogenous kynurenines as targets for drug discovery and development. *Nat. Rev. Drug Discovery* **2002**, *1*, 609–620.

(20) Macchiarulo, A.; Camaioni, E.; Nuti, R.; Pellicciari, R. Highlights at the gate of tryptophan catabolism: a review on the mechanisms of activation and regulation of indoleamine 2,3-dioxygenase (IDO), a novel target in cancer disease. *Amino Acids* **2009**, *37*, 219–229.

(21) Bessede, A.; Gargaro, M.; Pallotta, M. T.; Matino, D.; Servillo, G.; Brunacci, C.; Bicciato, S.; Mazza, E. M.; Macchiarulo, A.; Vacca, C.; Iannitti, R.; Tissi, L.; Volpi, C.; Belladonna, M. L.; Orabona, C.; Bianchi, R.; Lanz, T. V.; Platten, M.; Della Fazia, M. A.; Piobbico, D.; Zelante, T.; Funakoshi, H.; Nakamura, T.; Gilot, D.; Denison, M. S.; Guillemin, G. J.; DuHadaway, J. B.; Prendergast, G. C.; Metz, R.; Geffard, M.; Boon, L.; Pirro, M.; Iorio, A.; Veyret, B.; Romani, L.; Grohmann, U.; Fallarino, F.; Puccetti, P. Aryl hydrocarbon receptor control of a disease tolerance defence pathway. *Nature* **2014**, *511*, 184–190.

(22) Tokuriki, N.; Tawfik, D. S. Protein dynamism and evolvability. *Science* **2009**, *324*, 203–207.

(23) Urban, J. D.; Clarke, W. P.; von Zastrow, M.; Nichols, D. E.; Kobilka, B.; Weinstein, H.; Javitch, J. A.; Roth, B. L.; Christopoulos, A.; Sexton, P. M.; Miller, K. J.; Spedding, M.; Mailman, R. B. Functional selectivity and classical concepts of quantitative pharmacology. *J. Pharmacol. Exp. Ther.* **2007**, *320*, 1–13.

(24) Key, J.; Scheuermann, T. H.; Anderson, P. C.; Daggett, V.; Gardner, K. H. Principles of ligand binding within a completely buried cavity in HIF2alpha PAS-B. *J. Am. Chem. Soc.* **2009**, *131*, 17647–17654.

(25) Erbel, P. J.; Card, P. B.; Karakuzu, O.; Bruick, R. K.; Gardner, K. H. Structural basis for PAS domain heterodimerization in the basic helix–loop–helix-PAS transcription factor hypoxia-inducible factor. *Proc. Natl. Acad. Sci. USA* **2003**, *100*, 15504–15509.

(26) Razeto, A.; Ramakrishnan, V.; Litterst, C. M.; Giller, K.; Griesinger, C.; Carlomagno, T.; Lakomek, N.; Heimburg, T.; Lodrini, M.; Pfitzner, E.; Becker, S. Structure of the NCoA-1/SRC-1 PAS-B domain bound to the LXXLL motif of the STAT6 transactivation domain. *J. Mol. Biol.* **2004**, *336*, 319–29.

(27) Card, P. B.; Erbel, P. J.; Gardner, K. H. Structural basis of ARNT PAS-B dimerization: use of a common beta-sheet interface for hetero- and homodimerization. *J. Mol. Biol.* **2005**, *353*, 664–677.

(28) Scheuermann, T. H.; Tomchick, D. R.; Machius, M.; Guo, Y.; Bruick, R. K.; Gardner, K. H. Artificial ligand binding within the HIF2alpha PAS-B domain of the HIF2 transcription factor. *Proc. Natl. Acad. Sci. USA* **2009**, *106*, 450–455.

(29) George Priya Doss, C.; Sethumadhavan, R. Computational and structural analysis of deleterious functional SNPs in ARNT oncogene. *Interdiscip. Sci.* **2009**, *1*, 220–228.

(30) Zhu, J.; Martinez-Yamout, M.; Cardoso, R.; Yan, J.; Love, R. A.; Grodsky, N.; Brooun, A.; Dyson, H. J. Homodimerization of the PAS-B domains of hypoxia-inducible factors. *J. Phys. Chem. B* **2012**, *116*, 6960–6965.

(31) Pandini, A.; Denison, M. S.; Song, Y.; Soshilov, A. A.; Bonati, L. Structural and functional characterization of the aryl hydrocarbon receptor ligand binding domain by homology modeling and mutational analysis. *Biochemistry* **2007**, *46*, 696–708.

(32) Bisson, W. H.; Koch, D. C.; O'Donnell, E. F.; Khalil, S. M.; Kerkvliet, N. I.; Tanguay, R. L.; Abagyan, R.; Kolluri, S. K. Modeling of the aryl hydrocarbon receptor (AhR) ligand binding domain and its utility in virtual ligand screening to predict new AhR ligands. *J. Med. Chem.* **2009**, *52*, 5635–5641.

(33) Jogalekar, A. S.; Reiling, S.; Vaz, R. J. Identification of optimum computational protocols for modeling the aryl hydrocarbon receptor (AHR) and its interaction with ligands. *Bioorg. Med. Chem. Lett.* **2010**, *20*, 6616–6619.

(34) Pandini, A.; Soshilov, A. A.; Song, Y.; Zhao, J.; Bonati, L.; Denison, M. S. Detection of the TCDD binding-fingerprint within the Ah receptor ligand binding domain by structurally driven mutagenesis and functional analysis. *Biochemistry* **2009**, *48*, 5972–83.

(35) Goodale, B. C.; La Du, J. K.; Bisson, W. H.; Janszen, D. B.; Waters, K. M.; Tanguay, R. L. AHR2 mutant reveals functional diversity of aryl hydrocarbon receptors in zebrafish. *PLoS One* **2012**, *7*, e29346.

(36) Cavasotto, C. N.; Phatak, S. S. Homology modeling in drug discovery: current trends and applications. *Drug Discovery Today* **2009**, *14*, 676–683.

(37) Motto, I.; Bordogna, A.; Soshilov, A. A.; Denison, M. S.; Bonati, L. New aryl hydrocarbon receptor homology model targeted to improve docking reliability. *J. Chem. Inf. Model.* **2011**, *51*, 2868–2881.

(38) Cao, F.; Li, X.; Ye, L.; Xie, Y.; Wang, X.; Shi, W.; Qian, X.; Zhu, Y.; Yu, H. Molecular docking, molecular dynamics simulation, and structure-based 3D-QSAR studies on the aryl hydrocarbon receptor agonistic activity of hydroxylated polychlorinated biphenyls. *Environ. Toxicol. Pharmacol.* **2013**, *36*, 626–635.

(39) Salzano, M.; Marabotti, A.; Milanesi, L.; Facchiano, A. Human aryl-hydrocarbon receptor and its interaction with dioxin and physiological ligands investigated by molecular modelling and docking simulations. *Biochem. Biophys. Res. Commun.* **2011**, *413*, 176–181.

(40) Davis, I. W.; Murray, L. W.; Richardson, J. S.; Richardson, D. C. MOLPROBITY: structure validation and all-atom contact analysis for nucleic acids and their complexes. *Nucleic Acids Res.* **2004**, *32*, W615–619.

(41) Eisenberg, D.; Luthy, R.; Bowie, J. U. VERIFY3D: assessment of protein models with three-dimensional profiles. *Methods Enzymol.* **1997**, *277*, 396–404.

(42) Laskowski, R. A.; Rullmann, J. A.; MacArthur, M. W.; Kaptein, R.; Thornton, J. M. AQUA and PROCHECK-NMR: programs for checking the quality of protein structures solved by NMR. *J. Biomol. NMR* **1996**, *8*, 477–86.

(43) Halgren, T. A. Identifying and characterizing binding sites and assessing druggability. *J. Chem. Inf. Model.* **2009**, *49*, 377–89.

(44) Bochevarov, A. D.; Harder, E.; Hughes, T. F.; Greenwood, J. R.; Braden, D. A.; Philipp, D. M.; Rinaldo, D.; Halls, M. D.; Zhang, J.; Friesner, R. A. Jaguar: A high-performance quantum chemistry software program with strengths in life and materials sciences. *Int. J. Quantum Chem.* **2013**, *113*, 2110–2142.

(45) Cho, A. E.; Guallar, V.; Berne, B. J.; Friesner, R. Importance of accurate charges in molecular docking: quantum mechanical/molecular mechanical (QM/MM) approach. *J. Comput. Chem.* **2005**, *26*, 915–931.

(46) Kräutler, V.; Van Gunsteren, W. F.; Hünenberger, P. H. A fast SHAKE algorithm to solve distance constraint equations for small molecules in molecular dynamic simulations. *J. Comput. Chem.* **2001**, *22*, 501–508.

(47) Wisler, J. W.; Xiao, K.; Thomsen, A. R.; Lefkowitz, R. J. Recent developments in biased agonism. *Curr. Opin. Cell Biol.* **2014**, *27*, 18–24.

(48) De Bosscher, K. Selective Glucocorticoid Receptor modulators. *J. Steroid Biochem. Mol. Biol.* **2010**, *120*, 96–104.

(49) DuSell, C. D.; Nelson, E. R.; Wang, X.; Abdo, J.; Modder, U. I.; Umetani, M.; Gesty-Palmer, D.; Javitt, N. B.; Khosla, S.; McDonnell, D. P. The endogenous selective estrogen receptor modulator 27-hydroxycholesterol is a negative regulator of bone homeostasis. *Endocrinology* **2010**, *151*, 3675–3685.

(50) Connor, C. E.; Norris, J. D.; Broadwater, G.; Willson, T. M.; Gottardis, M. M.; Dewhirst, M. W.; McDonnell, D. P. Circumventing tamoxifen resistance in breast cancers using antiestrogens that induce unique conformational changes in the estrogen receptor. *Cancer Res.* **2001**, *61*, 2917–2922.

(51) Kazmin, D.; Prytkova, T.; Cook, C. E.; Wolfinger, R.; Chu, T. M.; Beratan, D.; Norris, J. D.; Chang, C. Y.; McDonnell, D. P. Linking ligand-induced alterations in androgen receptor structure to differential gene expression: a first step in the rational design of selective androgen receptor modulators. *Mol. Endocrinol.* **2006**, *20*, 1201–1217.

(52) Safe, S.; McDougal, A. Mechanism of action and development of selective aryl hydrocarbon receptor modulators for treatment of hormone-dependent cancers (Review). *Int. J. Oncol.* **2002**, *20*, 1123–1128.

(53) Matikainen, T.; Perez, G. I.; Jurisicova, A.; Pru, J. K.; Schlezinger, J. J.; Ryu, H. Y.; Laine, J.; Sakai, T.; Korsmeyer, S. J.; Casper, R. F.; Sherr, D. H.; Tilly, J. L. Aromatic hydrocarbon receptor-driven Bax gene expression is required for premature ovarian failure caused by biohazardous environmental chemicals. *Nat. Genet.* **2001**, *28*, 355–360.

(54) Gouedard, C.; Barouki, R.; Morel, Y. Dietary polyphenols increase paraoxonase 1 gene expression by an aryl hydrocarbon receptor-dependent mechanism. *Mol. Cell. Biol.* **2004**, *24*, 5209–5222.

(55) Zhao, B.; Degroot, D. E.; Hayashi, A.; He, G.; Denison, M. S. CH223191 is a ligand-selective antagonist of the Ah (Dioxin) receptor. *Toxicol. Sci.* **2010**, *117*, 393–403.